

^{13}C NMR (90 MHz, CD_2Cl_2): δ 213.1 (Zr-C-), 161.5, 145.4, 142.6, 134.4, 121.6, 120.9, 116.5 (Cp), 21.4 (Me), 14.6 (Me).

FTIR (KBr pellet, cm^{-1}): $\nu_{\text{C-C}}$ 1534.9.

Acknowledgment. This work was supported by DOE Grant DE-FG02-88ER13935, NSF Grant CHE8816445, the

Volkswagen-Stiftung, and the Iowa EARDA program. NMR spectra were obtained in the University of Iowa High-field NMR Facility. R.F.J. gratefully acknowledges a Sloan Foundation Research Fellowship (1989-91) and Union Carbide Research Innovation Awards (1989, 1990).

Studies of the Oxidatively Promoted Carbonylation of $\eta\text{-Cp}(\text{CO})(\text{L})\text{FeMe}$ in Methylene Chloride. Applications of the Quantitative Analysis of Ligand Effects

Alfred Prock,* Warren P. Giering,* Jack E. Greene,[†] Randy E. Meirowitz, Steven L. Hoffman,[†] David C. Woska,[†] Matthew Wilson,[†] Richard Chang,[†] Jianxiang Chen, Roy H. Magnuson, and Klaas Eriks

Department of Chemistry, Arthur G. B. Metcalf Center for Science and Engineering, Boston University, Boston, Massachusetts 02215

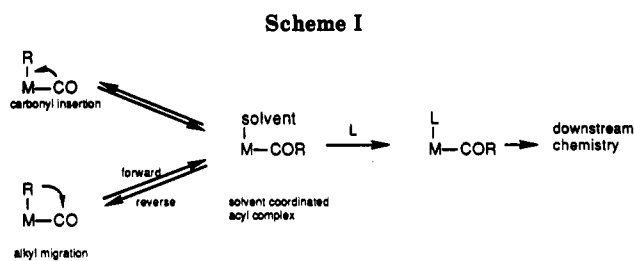
Received November 28, 1990

The carbonylation of $\eta\text{-Cp}(\text{CO})(\text{L})\text{FeMe}^+$ ($\text{L} = \text{PPhMe}_2, \text{PEt}_3, \text{PPh}_2\text{Me}, \text{PEt}_2\text{Ph}, \text{PPh}_2\text{Et}, \text{P}(p\text{-MeOPh})_3, \text{P}(p\text{-MePh})_3, \text{PPh}_3, \text{P}(p\text{-FPh})_3, \text{P}(p\text{-ClPh})_3, \text{P}(p\text{-CF}_3\text{Ph})_3, \text{PPh}_2\text{Cy}, \text{PPhCy}_2, \text{PCy}_3$) in methylene chloride has been studied by a combination of kinetic, stereochemical, isotopic labeling, ligand effect, and electrochemical experiments. Redox-catalyzed (ferrocenium tetrafluoroborate) carbonylation of (+)- $\eta\text{-Cp}(\text{CO})(\text{PPh}_3)\text{FeMe}$ gives racemic $\eta\text{-Cp}(\text{CO})(\text{PPh}_3)\text{FeCOMe}$. The results of control experiments suggest that the racemization is attributable to the configurational instability of $\eta\text{-Cp}(\text{CO})(\text{PPh}_3)\text{FeMe}^+$. The redox-catalyzed carbonylation of $\eta\text{-Cp}(\text{CO})(\text{PPh}_3)\text{FeMe}$ under 1 atm of ^{13}C O affords $\eta\text{-Cp}(^{13}\text{C})\text{O}(\text{PPh}_3)\text{FeCOMe}$. The rate of the electrochemically promoted carbonylation of $\eta\text{-Cp}(\text{CO})(\text{L})\text{FeMe}$ is independent of the concentration of the starting complex, carbon monoxide, and the supporting electrolyte, tetrabutylammonium hexafluorophosphate (TBAH). Kinetic data for the carbonylation of $\eta\text{-Cp}(\text{CO})(\text{L})\text{FeMe}^+$, which is first order in complex and zero order in carbon monoxide, were obtained by computer simulation analysis of cyclic and square-wave voltammetry data. Analysis of the data for $\text{L} = \text{P}(p\text{-ClPh})_3$ and $\text{P}(p\text{-CF}_3\text{Ph})_3$ reveals enthalpies of activation ($\Delta H^\ddagger = 7.8 \pm 2.0, 6.7 \pm 0.8$ kcal/mol) and entropies of activation ($\Delta S^\ddagger = -23 \pm 7, -25 \pm 3$ eu), respectively. Quantitative analysis of the ligand effect (QALE) data shows that the carbonylation of $\eta\text{-Cp}(\text{CO})(\text{L})\text{FeMe}^+$ is accelerated by poorer electron-donor ligands; the steric profile shows a region of steric inhibition for small ligands with a steric threshold at 150° after which the rate of reaction rises rapidly. Analysis of the E° values for the $\eta\text{-Cp}(\text{CO})(\text{L})\text{FeMe}/\eta\text{-Cp}(\text{CO})(\text{L})\text{FeMe}^+$ couple also reveals a steric threshold at 150° .

Introduction

Because of its crucial position in the chemistry of carbon monoxide, the alkyl to acyl migratory insertion reaction is among the most studied of chemical processes.¹ The current view of this reaction is a composite picture derived from the results of studies of a number of systems (Scheme I). In particular, the kinetics, the nature of the carbonylation step (alkyl migration versus carbonyl insertion),² stereochemistry at both the metal² and the α -carbon of the alkyl group,³ and the effect of the electron-donor capacity of the alkyl group⁴ have received attention. It is now widely believed that many of the alkyl to acyl migratory insertion reactions are assisted by concomitant incorporation of a nucleophilic solute or solvent.⁵ The role of oxidation state of the central metal has been little studied, however, although it is known that the oxidation^{6,7} or reduction^{8,9} of alkylmetal carbonyls greatly accelerates the carbonylation of the metal-alkyl bond.

A number of years ago we reported that the iron(III) complex $\eta\text{-Cp}(\text{CO})(\text{PPh}_3)\text{FeMe}^+$ undergoes carbonylation at least 1 million times faster than the analogous iron(II) complex.^{6c} The origins of this high reactivity have been of interest for a number of years.¹⁰ Predicated by studies of the pyridine-induced rearrangement of $\eta\text{-Cp}(\text{CO})$ -



(PPh_3) FeMe^+ , Troglor^{10b} concluded that nucleophilic assistance might be important and that the heptacoordinate

(1) (a) Kihlman, E. J.; Alexander, J. J. *Coord. Chem. Rev.* **1980**, *33*, 195-225. (b) Calderazzo, F. *Angew. Chem., Int. Ed. Engl.* **1977**, *16*, 299-311. (c) Wojcicki, A. *Adv. Organomet. Chem.* **1973**, *11*, 87-145. (d) Collman, J. P.; Hegedus, L. S.; Norton, J. R.; Finke, R. G. *Principles and Applications of Organotransition Metal Chemistry*; University Science Books: Mill Valley, CA, 1987.

(2) (a) Flood, T. C.; Jensen, J. E.; Statler, J. A. *J. Am. Chem. Soc.*, **1981**, *103*, 4410-14. (b) Flood, T. C.; Campbell, K. D. *J. Am. Chem. Soc.*, **1984**, *106*, 2853-60. (c) Calderazzo, F.; Noack, K. *J. Organomet. Chem.* **1967**, *10*, 101-104. (d) Brunner, H.; Vogt, H. *Angew. Chem., Int. Ed. Engl.* **1981**, *20*, 405.

(3) (a) Nicholas, K. M.; Rosenblum, M. *J. Am. Chem. Soc.* **1973**, *95*, 4449-4450. (b) Bock, R. L.; Boschetto, J. R.; Rasmussen, J. P.; Demers, J. P.; Whitesides, G. M. *J. Am. Chem. Soc.* **1980**, *102*, 6887.

(4) Connor, J. A.; Zafarani-Moattar, M. T.; Bickerton, J.; El Saied, N. L.; Suradi, S.; Carson, R.; Al Takhin, G.; Skinner, H. A. *Organometallics* **1982**, *1*, 1166.

[†] Undergraduate research participant.

complex $\eta\text{-Cp}(\text{CO})(\text{PPh}_3)(\text{py})\text{FeMe}^+$ is a direct progenitor of $\eta\text{-Cp}(\text{PPh}_3)(\text{py})\text{FeCOMe}^+$. This seems quite reasonable in view of the susceptibility of 17-electron organometallic species to attack by nucleophilic reagents.¹¹ In addition, it has been suggested, based on theoretical calculations, that the transition state of the alkyl to acyl migratory insertion reaction for $\text{MeMn}(\text{CO})_5$ is electron deficient at the metal.¹² This electron deficiency is enhanced in an electron-deficient cation radical and thereby facilitates the incorporation of the solvent.

In this paper, we present evidence from kinetic, stereochemical, isotopic labeling, solvent, and ligand effect studies that indicate the carbonylation of $\eta\text{-Cp}(\text{L})(\text{CO})\text{FeMe}^+$ is nucleophilically assisted.

Experimental Section

General Procedures. All manipulations and preparations were carried out under argon using standard techniques. All glassware used in electrochemical studies were baked and removed from the oven immediately prior to use. Methylene chloride (HPLC grade) was distilled twice from phosphorus pentoxide immediately prior to use.¹³ Anhydrous diethyl ether was distilled from sodium benzophenone ketyl. Tetrabutylammonium hexafluorophosphate (TBAH) was recrystallized from ethyl acetate. All phosphines and phosphites as well as methyl iodide, dimethyl sulfate, and ferrocene were obtained from commercial sources and were used without further purification. $\eta\text{-Cp}(\text{CO})_2\text{FeMe}$ was prepared by sodium amalgam reduction of $[\eta\text{-Cp}(\text{CO})_2\text{Fe}]_2$ in tetrahydrofuran followed by alkylation with dimethyl sulfate. Infrared and NMR spectra were measured on a Perkin-Elmer Model 1800 FTIR and a JEOL 270 NMR spectrometers, respectively. Electrochemical measurements were performed on either an EG&G PAR Model 174 polarographic analyzer or an EG&G PAR 273 potentiostat/galvanostat controlled by a Compuadd 286 computer. A standard three-electrode cell equipped with a platinum disk electrode and an SCE reference electrode (174A polarographic analyzer) or a pseudoreference platinum wire electrode (Model 273 potentiostat/galvanostat) was employed. Simulations were carried out on IBM 7090 computer using codes written in our laboratories. (See the text and supplementary material.)

The phosphine methyl complexes, $\eta\text{-Cp}(\text{CO})(\text{L})\text{FeMe}$, were prepared either by methylation of $\eta\text{-Cp}(\text{CO})(\text{L})\text{FeI}$ with me-

thyllithium or by photolysis of a refluxing acetonitrile solution of $\eta\text{-Cp}(\text{CO})_2\text{FeMe}$ in the presence of about a 2–3-fold excess of phosphine. Regardless of the mode of preparation, the $\eta\text{-Cp}(\text{CO})(\text{L})\text{FeMe}$ complexes were purified by chromatography on neutral or basic activity II alumina. We found the resulting product tended to be contaminated with traces of free phosphine and phosphine oxide (via ³¹P NMR spectroscopy), which were removed by dissolving the sample in a small amount of benzene and adding methyl iodide. After the reaction mixture had been allowed to stand overnight under argon, its volume was reduced by rotary evaporation and then percolated through alumina. The resulting materials were free of phosphine, phosphine oxides, and phosphonium iodides. All materials were characterized by ³¹P and ¹H NMR spectroscopy and IR spectroscopy.

Determination of the Concentration of CO in Methylene Chloride Containing 0.1 M TBAH at 0 °C. The redox-catalyzed (ferrocenium hexafluorophosphate, 5 mol % based on complex) carbonylation of 0.10 g of $\eta\text{-Cp}(\text{CO})(\text{PPh}_3)\text{FeMe}$ in methylene chloride saturated with carbon monoxide at 0 °C was shown to effect the essentially complete (93%) conversion of the methyl complex to $\eta\text{-Cp}(\text{CO})(\text{PPh}_3)\text{FeCOMe}$ after 20 min. This reaction was used to measure the concentration of CO in methylene chloride containing 0.1 M TBAH at 0 °C. Solutions of $\eta\text{-Cp}(\text{CO})(\text{PPh}_3)\text{FeMe}$ that ranged in concentration from 15 to 25 mM were prepared in centrifuge tubes and cooled to 0 °C. The solutions were then saturated with CO. The remaining CO in the dead space at the top of the tube was flushed quickly with argon, and the tube was capped. The carbonylation was initiated by injecting 5 mol % (based on complex) ferrocenium hexafluorophosphate as a 0.091 M solution in acetone. The carbonylation was allowed to proceed for periods ranging from 20 min to 14 h. (The results were found to be independent of time after 20 min.) The solutions were purged with argon, and then a 1-mL sample was transferred to an electrochemical cell. The relative concentrations of $\eta\text{-Cp}(\text{CO})(\text{PPh}_3)\text{FeMe}$ and $\eta\text{-Cp}(\text{CO})(\text{PPh}_3)\text{FeCOMe}$ were determined by square-wave voltammetry. When material, which was lost to oxidation by the catalyst, was taken into account, the concentration of CO was calculated to be 7.9 (± 0.3) mM based on the analysis of 10 samples.

Stereochemical Experiments with (+)- $\eta\text{-Cp}(\text{CO})(\text{PPh}_3)\text{FeMe}$. (+)- $\eta\text{-Cp}(\text{CO})(\text{PPh}_3)\text{FeMe}$ was prepared by the method of Flood^{2a} ($[\alpha]_D = +90^\circ$, CH_2Cl_2 , c 0.001, which agrees with the literature value^{2a}). (+)- $\eta\text{-Cp}(\text{CO})(\text{PPh}_3)\text{FeMe}$ (10.6 mg, 2.49×10^{-2} mmol) was placed in a 25-mL volumetric flask and diluted to 9.96×10^{-4} M with CH_2Cl_2 . Ferrocenium tetrafluoroborate (6.8 mg, 2.5×10^{-2} mmol) was placed in another 25-mL volumetric flask and diluted to 1.0×10^{-3} M with CH_2Cl_2 . A 1.0-mL polarimeter cell was filled with (+)- $\eta\text{-Cp}(\text{CO})(\text{PPh}_3)\text{FeMe}$ stock solution and the optical rotation determined ($[\alpha]_D = +90^\circ$, CH_2Cl_2 , c 0.001). This solution was then placed in the volumetric flask, and the entire solution was purged with carbon monoxide over a 10-min period. At the end of this period, 1.25 mL of the ferrocenium tetrafluoroborate solution was added by syringe (5 mol %). A 1.0-mL aliquot of this solution was checked for optical rotation. It was determined to have lost all optical activity.

Another solution of (+)- $\eta\text{-Cp}(\text{CO})(\text{PPh}_3)\text{FeMe}$ was prepared at the same concentration as the original stock solution. This solution was purged with argon for 10 min. Ferrocenium tetrafluoroborate solution (1.25 mL, 5 mol %) was added by syringe. This mixture was determined to have lost optical activity.

Redox-Catalyzed Carbonylation of $\eta\text{-Cp}(\text{CO})(\text{PPh}_3)\text{FeMe}$ with ¹³CO. A 20-mL portion of a methylene chloride solution of $\eta\text{-Cp}(\text{CO})(\text{PPh}_3)\text{FeMe}$ was injected into a sealed flask containing 250 mL of ¹³CO at 1 atm. The solution was then cooled in an ice bath and allowed to equilibrate with the ¹³CO for 20 min with constant shaking. The oxidant was prepared by dissolving 3 mg of ferrocenium hexafluorophosphate in 10 mL of CH_2Cl_2 that had been purged with argon. Of the oxidant solution, 2 mL was injected into the flask. The solution was then swirled gently for 20 min, and after the contents were warmed to room temperature, it was rotary evaporated. The residue was separated on a 1 cm \times 14 cm column of activity III neutral alumina. The starting material was collected as the first red-orange band, which was eluted with petroleum ether. $\eta\text{-Cp}(\text{CO})(\text{PPh}_3)\text{Fe}(\text{COMe})$ was collected as the second yellow band, which was eluted with a 70/30 mixture of benzene and petroleum ether. The ¹³C NMR

(5) (a) Webb, S. L.; Giandomenico, C. M.; Halpern, J. *J. Am. Chem. Soc.* 1986, 108, 345–47. (b) Wax, M. J.; Bergman, R. G. *J. Am. Chem. Soc.* 1981, 103, 7028. (c) Martin, B. D.; Warner, K. E.; Norton, J. R. *J. Am. Chem. Soc.* 1986, 108, 33–39.

(6) (a) Magnuson, R. H.; Zulu, S. J.; T'sai, W.-M.; Giering, W. P. *J. Am. Chem. Soc.* 1980, 102, 6887–88. (b) Magnuson, R. H.; Meirowitz, R. E.; Zulu, S. J.; Giering, W. P. *J. Am. Chem. Soc.* 1982, 104, 5790–91. (c) Magnuson, R. H.; Meirowitz, R. E.; Zulu, S. J.; Giering, W. P. *Organometallics* 1983, 2, 460–62. (d) Javaheri, S.; Giering, W. P.; *Organometallics* 1984, 3, 1927. (e) Golovin, M. N.; Meirowitz, R. E.; Rahman, Md. M.; Liu, H.-Y.; Prock, A.; Giering, W. P. *Organometallics* 1987, 6, 2285–89. (f) Liu, H.-Y.; Fertal, D.; Tracey, A. A.; Eriks, K.; Prock, A.; Giering, W. P. *Organometallics* 1989, 8, 1454–58. (g) Tracey, A. A.; Eriks, K.; Prock, A.; Giering, W. P. *Organometallics* 1990, 9, 1399.

(7) (a) Anderson, S. N.; Fong, C. W.; Johnson, M. D. *J. Chem. Soc., Chem. Commun.* 1973, 163. (b) Slack, D. A.; Baird, M. C. *J. Am. Chem. Soc.* 1976, 98, 5539–46. (c) Rogers, W.; Page, J. A.; Baird, M. C. *J. Organomet. Chem.* 1978, 156, C37–C42. (d) Rogers, W. N.; Page, J. A.; Baird, M. C. *Inorg. Chem.* 1981, 20, 3521–28. (e) Klingler, R. J.; Kochi, J. K. *Organometallics* 1980, 202, 49–63. (f) Reger, D. L.; Mintz, E. *Organometallics* 1984, 3, 1759–61. (g) Bly, R. S.; Silverman, G. S.; Hossain, M. M.; Bly, R. K. *Organometallics* 1984, 3, 642–44. (h) Bly, R. S.; Silverman, G. S.; Bly, R. K. *Organometallics* 1985, 4, 375–83. (i) Sheridan, J. B.; Han, S. H.; Geoffrey, G. L. *J. Am. Chem. Soc.* 1987, 109, 8097.

(8) Donovan, B. T.; Geiger, W. E. *Organometallics* 1990, 9, 865.

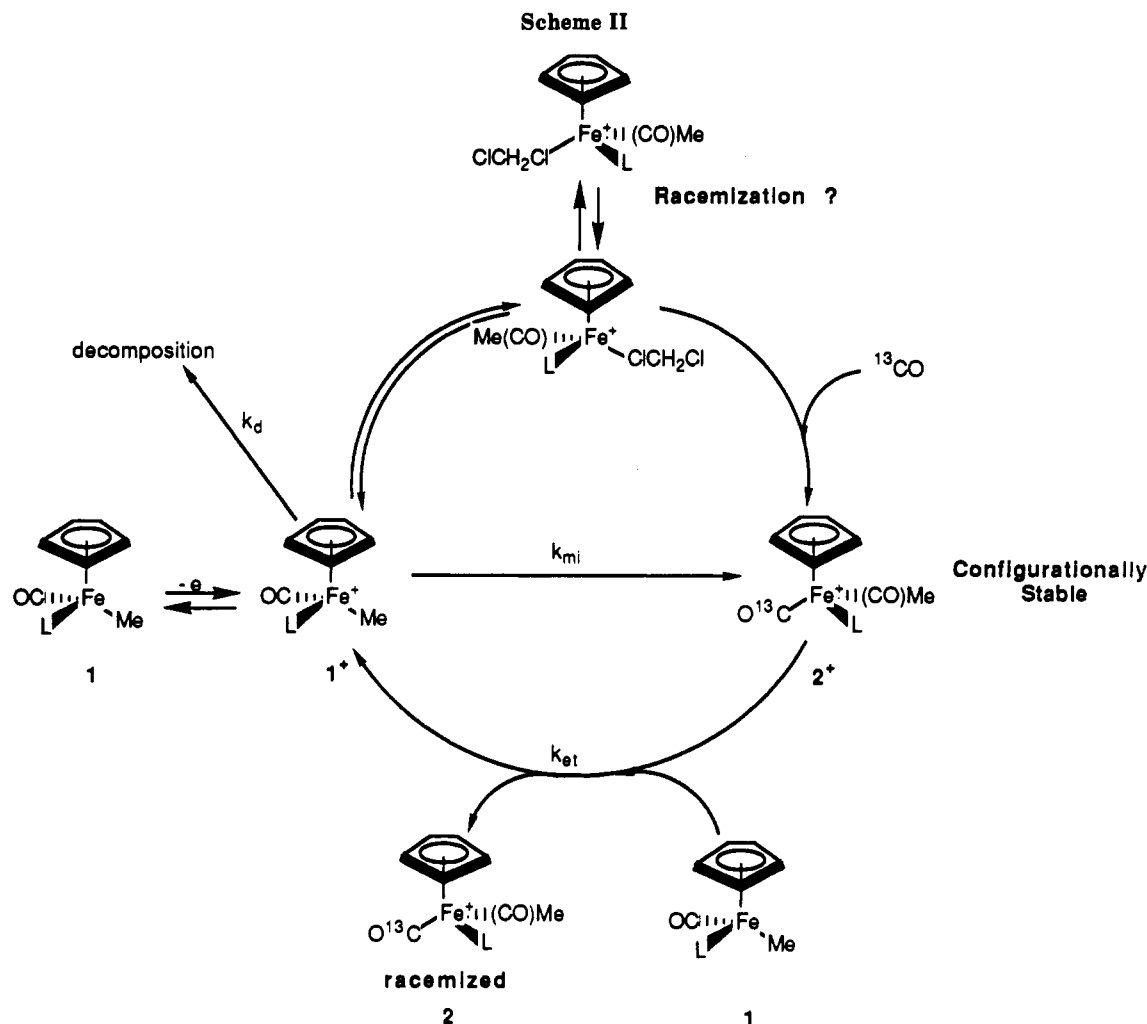
(9) Miholova, D.; Vleck, A. A. *J. Organomet. Chem.* 1982, 240, 413.

(10) (a) Doxsee, K. M.; Grubbs, R. H.; Anson, F. C. *J. Am. Chem. Soc.* 1984, 106, 7819. (b) Therien, M. J.; Trogler, W. C. *J. Am. Chem. Soc.* 1987, 109, 5127. (c) Reger, D. L.; Mintz, E.; Lebioda, L. *J. Am. Chem. Soc.* 1986, 108, 1940.

(11) Baker, R. T.; Calabrese, J. C.; Krusic, P. J.; Therien, M. J.; Trogler, W. C. *J. Am. Chem. Soc.* 1988, 110, 8392.

(12) Axe, F. U.; Marynick, D. S. *J. Am. Chem. Soc.* 1988, 110, 3728.

(13) Zizelman, P. M.; Amatore, C.; Kochi, J. K. *J. Am. Chem. Soc.* 1984, 106, 3771.



spectrum of the product, $\eta\text{-Cp}(^{13}\text{CO})(\text{PPh}_3)\text{FeCOMe}$, and residual methyl complex demonstrated that only the terminal carbonyl position of the acetyl complex was labeled. There was no indication of the label appearing in the terminal carbonyl ligand of the methyl complex or in the acyl carbonyl of the acetyl complex.

Determination of the Rates of Carbonylation of $\eta\text{-Cp}(\text{CO})(\text{L})\text{FeMe}$ by Electrochemical Methods. In a typical experiment, 2–10 mg of $\eta\text{-Cp}(\text{CO})(\text{L})\text{FeMe}$ was dissolved in 25 mL of argon-purged methylene chloride containing 0.1 M TBAH at 0 °C. Cyclic (CV) and square-wave (SW) voltammograms were measured at various scan rates to determine the decomposition rate constants of $\eta\text{-Cp}(\text{CO})(\text{L})\text{FeMe}^+$, the heterogeneous rate constants, and transfer coefficients. The solution was then saturated with CO (approximately 15 min). Mixtures of argon and carbon monoxide were used to vary the concentration of CO in the reaction mixtures. Variable-temperature experiments were performed in acetonitrile and carbon tetrachloride slush baths. Data suitable for computer simulation were readily obtained from square-wave voltammetry with scan rates ranging from 0.002 to 0.5 V s⁻¹. Scans started at negative potentials and moved toward more positive potentials.

Computer Simulation of Electrochemical Experiments. Determination of k_{mi} for $\eta\text{-Cp}(\text{CO})(\text{L})\text{FeMe}$. The simulation code for square-wave analysis is based on the chemistry shown in Scheme II. The electron-transfer rate constant, k_{et} , is taken to be very large. In order to avoid the need for very small time increments, we assume k_{et} to be infinite and consider two cases. Case 1 is when the concentration of species 1 is greater than species 2⁺. Case 2 is the opposite. This method is similar to that of Kochi,¹³ except that we need to use the second case as well.

Case 1 is dealt with by setting $\partial[2^+]/\partial t$ to zero. This leads to the expression

$$D\partial^2[2^+]/\partial x^2 = -k_{\text{mi}}[\text{CO}][1^+] + k_{\text{et}}[2^+][1^+] \quad (1)$$

On incorporating this expression into the set of equations de-

scribing the scheme shown, we obtain a form suitable for numerical analysis:

$$\partial[1^+]/\partial t = D\partial^2[1^+]/\partial x^2 + D\partial^2[2^+]/\partial x^2 - k_{\text{d}}[1^+] \quad (2)$$

$$\partial[1]/\partial t = D\partial^2[1]/\partial x^2 - D\partial^2[2^+]/\partial x^2 - k_{\text{mi}}[\text{CO}][1^+] \quad (3)$$

$$\partial[2]/\partial t = D\partial^2[2]/\partial x^2 + D\partial^2[2^+]/\partial x^2 + k_{\text{mi}}[\text{CO}][1^+] \quad (4)$$

For case 2 we set $\partial[1]/\partial t$ to zero. This leads to

$$D\partial^2[1]/\partial x^2 = k_{\text{et}}[2^+][1^+] \quad (5)$$

On incorporating as above, we get

$$\partial[1^+]/\partial t = D\partial^2[1^+]/\partial x^2 + D\partial^2[1]/\partial x^2 - k_{\text{mi}}[\text{CO}][1^+] - k_{\text{d}}[1^+] \quad (6)$$

$$\partial[2]/\partial t = D\partial^2[2]/\partial x^2 + D\partial^2[1]/\partial x^2 \quad (7)$$

$$\partial[2^+]/\partial t = D\partial^2[2^+]/\partial x^2 - D\partial^2[1]/\partial x^2 + k_{\text{mi}}[\text{CO}][1^+] \quad (8)$$

A decision is made at each step whether case 1 or 2 applies. A small discontinuity results on switching between cases, which is manifest in the computed current-potential curves as a somewhat sharp valley between the peaks representing the 1/1⁺ and 2/2⁺ couples. We were able to remedy this fully by a simple expedient. We inserted a branch such that when *both* species 2⁺ and 1 are present at very low concentration, the computation reverts, for a few steps only, to the original set of differential equations containing a large k_{et} around 3, expressed in the dimensionless variable $A = k_{\text{et}}[1^0]\Delta t$, where [1⁰] is the initial concentration of $\eta\text{-Cp}(\text{CO})(\text{PPh}_3)\text{Fe}(\text{Me})$ and Δt is the time interval. The result turns out to be *insensitive* to k_{et} in this range; moreover, this correction is strictly local and has virtually no effect on the remainder of the computation. It does, however, produce the proper shape and current ratio at the minimum.

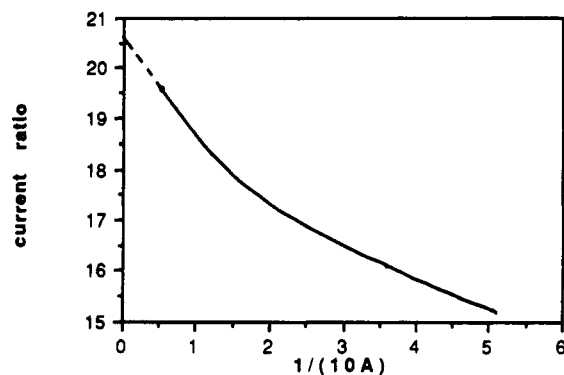


Figure 1. Peak current ratio, i_2/i_1 , for an experiment computed as a function of rate of electron transfer, k_{et} , expressed in dimensionless terms, $A = k_{et}[1^0]\Delta t$. See text for terms and definitions.

The computed ratio i_2/i_1 , of peak currents i_2 and i_1 near the reduction potentials of $\eta\text{-Cp}(\text{CO})(\text{L})\text{Fe}(\text{COMe})^+$ and $\eta\text{-Cp}(\text{CO})(\text{PPh}_3)\text{Fe}(\text{Me})^+$ for "infinite" k_{et} (vide supra) was compared to values of i_2/i_1 that we computed using a code written for finite k_{et} . This is shown in Figure 1. The maximum useable value of A is around 0.2 and corresponds to the left-hand point of the solid curve. The point for zero on the abscissa is the value computed for infinite k_{et} . The graph in Figure 1 indicates that the results for "infinite" k_{et} are indeed a reasonable extrapolation of results for finite k_{et} .

A common value of diffusion coefficient was employed for all species. Because the CO concentration was always at least a factor of 8 greater than the iron concentration, the error was expected to be negligible. This was checked by taking the diffusion coefficient for CO to be 2.5 times larger than the common D in the simulation. The difference was, indeed, insignificant.

The iron(II) methyl and acetyl species, both being stable, were examined individually by means of CV and SW methods. Since over a range of scan rates the current-potential curves for CV and SW depend somewhat differently on the heterogeneous rate constants, k/\sqrt{D} , and transfer coefficients, α , we could combine CV and SW methods in order to determine k/\sqrt{D} and α . We find the k/\sqrt{D} values to lie in the range from 0.7 to $2\text{ s}^{-1/2}\text{ cm}^{-1}$. We point out that these are effective rate constants, which also include the effect of finite solution resistance. Their errors are estimated to be no more than 10%, which (vide infra) introduces only a small uncertainty into the final result. This fortunate effect seems traceable to the virtually infinite k_{et} , which produces rather sharp peaks even for these k/\sqrt{D} values. The values of α lie between 0.40 and 0.50, with an uncertainty of 0.03. The decay rates of the oxidized forms, 1^+ and 2^+ , were obtained through CV methods. The decay rates of 1^+ were $0.01\text{--}0.12\text{ s}^{-1}$; those for 2^+ were even smaller. For simulation purposes, both associated errors were negligible. The redox potentials for the $1/1^+$ and $2/2^+$ couples are relative values, only, obtained with the use of a pseudo reference electrode.

The rate constant, k_{mi} , was then determined by fitting the peak current ratios (SW) from our kinetic data to the computed ones through a least-squares method.

Errors originate from sources including the following. Differences in measured peak potential for both SW and CV experiments are within 10 mV. When translated into a difference of reduction potentials, this causes no more than a 2.5% change in i_2/i_1 . Measured current ratios, i_2/i_1 and i_{min}/i_1 , are obtainable to within 3% error. The ratio i_{min}/i_1 is much less sensitive to scan rate, in agreement with computations. A change of 0.05 in both values of α causes a 1% change in the ratio. A 10% change in either heterogeneous rate constant causes a 3% change in the current ratio. When to these uncertainties are added the uncertainty from the least-squares fit of k_{mi} to the data for the range of scan rates employed, we arrive at an uncertainty of no more than 15% in k_{mi} . This suffices for present purposes but by no means represents the least error obtainable for this system by these electrochemical methods.

We have assumed equality of diffusion coefficients of all electrochemically active species in each experiment based on the

small differences in their molecular weights. Differences might arise owing to differing degree of solvation of various oxidation states even for a solvent of low polarity like methylene chloride. Accordingly, we repeated the simulations with an arbitrary value of 1.5 for the ratio of diffusion coefficients, $D(\text{reduced})/D(\text{oxidized})$. We took the same ratio for all corresponding oxidized and reduced species. We find that the quality of fit to experimental data deteriorates in comparison to results for equality of diffusion coefficients. Furthermore, the final result is rather insensitive to this ratio: the best fit values of k_{mi} change, but all in the same direction so that the relative change in any value of $\log k$ is no more than several percent of the range. We conclude that for this system equality of diffusion coefficients is a reasonable assumption. The code provided in the supplementary material is the version written for equal ratios of the diffusion coefficient. Numerical computation was done by means of the Adams-Moulton method, as previously described.⁶

Results

The high reactivity of $\eta\text{-Cp}(\text{CO})(\text{L})\text{FeMe}^+$ coupled with thermodynamic favorability of the carbonylation reaction in the iron(II) state and the more positive reduction potential of the $\eta\text{-Cp}(\text{CO})(\text{L})\text{FeCOMe}/\eta\text{-Cp}(\text{CO})(\text{L})\text{FeCOMe}^+$ couple sets the stage for the facile redox-catalyzed carbonylation of $\eta\text{-Cp}(\text{CO})(\text{L})\text{FeMe}$ as described in Scheme II. On a preparative scale, the reaction is very efficient as evidenced by the ferrocenium-catalyzed conversion of $\eta\text{-Cp}(\text{CO})(\text{PPh}_3)\text{FeMe}$ to $\eta\text{-Cp}(\text{CO})(\text{PPh}_3)\text{FeCOMe}$, which is essentially quantitative (93%) under 1 atm of CO at 0 °C. We exploited this chemistry to determine electrochemically the migratory rate constant, k_{mi} , for the carbonylation of the iron(III) complexes, $\eta\text{-Cp}(\text{CO})(\text{L})\text{FeCOMe}^+$, in methylene chloride (Scheme II).

The redox-catalyzed carbonylation of $\eta\text{-Cp}(\text{CO})(\text{L})\text{FeMe}$ is readily observed and studied by electrochemical methods. Thus, when CV's of $\eta\text{-Cp}(\text{CO})(\text{L})\text{FeMe}$ are measured under an argon atmosphere, a single set of waves is observed. The cathodic return waves are attenuated, indicating that the cation radicals, $\eta\text{-Cp}(\text{CO})(\text{L})\text{FeMe}^+$, are somewhat unstable on the time scale of the experiment. This is particularly noticeable for the complexes bearing the more electronegative phosphine ligands. The cyclic voltammograms change dramatically when measured under an atmosphere of carbon monoxide. For example, under these conditions anodic waves for both the methyl complex, $\eta\text{-Cp}(\text{CO})(\text{L})\text{FeMe}$, as well as the acetyl complex, $\eta\text{-Cp}(\text{CO})(\text{L})\text{FeCOMe}$, are observed. The cyclic voltammogram is scan rate dependent, with the relative current of the methyl anodic wave decreasing with decreasing scan rate and the relative current of the acetyl anodic wave increasing with decreasing scan rate. The rate constants, k_{mi} , for the carbonylation of $\eta\text{-Cp}(\text{CO})(\text{L})\text{FeMe}^+$ were extracted from CV and SW data by computer simulation methods. Experimental and simulated SW's are displayed in Figure 2. These rate constants, which were measured for a variety of L are displayed in Table I. In methylene chloride, the rates of carbonylation are independent of [CO] (0.25–1.0 atm), $[\eta\text{-Cp}(\text{CO})(\text{L})\text{FeMe}]$ (0.25–1.0 mM), and [TBAH] (0.05–0.2 M) (eq 9).¹⁴ The activation pa-

(14) Early experiments using methylene chloride distilled from calcium hydride showed the reaction to be first order in carbon monoxide with a rate constant of $410\text{ m}^{-1}\text{ s}^{-1}$ for $\text{L} = \text{PPh}_3$.^{6c} Our recent work shows that the early kinetic data was influenced by a nucleophilic impurity in the methylene chloride that was not readily removed by calcium hydride. (We will discuss nucleophilic catalysis in subsequent sections of this paper.) The experimental results discussed herein were obtained with use of methylene chloride that had been distilled twice from phosphorus pentoxide. Subsequent distillation from calcium hydride had no effect on the kinetic data.

(15) Bartik, T.; Himmler, T.; Schulte, H.-G.; Seevogel, K. *J. Organomet. Chem.* 1984, 272, 29.

(16) Tolman, C. A. *Chem. Rev.* 1977, 77, 313.

Table I. Stereoelectronic Parameters for Phosphine Ligands and Kinetic Data for the Carbonylation of η -Cp(CO)(L)FeMe⁺ in Methylene Chloride

ligand	χ^a	θ^b	k_{mi}^c	$E^{\circ d}$
PMe ₃	8.55	118	0.068	-486
PMe ₂ Ph	10.6	122	0.071	-443
PEt ₃	6.3	132	0.005	-522
PMePh ₂	12.1	136	0.055	-403
PEtPh ₂	11.3	140	0.039	-425
P(<i>p</i> -MeOPh) ₃	10.5	145	0.036	-451
P(<i>p</i> -MePh) ₃	11.5	145	0.043	-430
PPh ₃	13.25	145	0.067	-384
P(<i>p</i> -PPh) ₃	15.0	145	0.066	
P(<i>p</i> -ClPh) ₃	16.8	145	0.182	-280
P(<i>p</i> -CF ₃ Ph) ₃	22.5	145	0.474	-205
PCyPh ₂	9.3	153	0.020	-457
PCy ₂ Ph	5.35	161	0.027	-528
PCy ₃	1.4	170	0.024	-602

^a χ values (cm⁻¹) are taken from data reported by Bartik et al.¹⁵
^b Cone angles (deg) are taken from data reported by Tolman or calculated from data provided therein.¹⁶ ^c First-order rate constants (s⁻¹) for the carbonylation of η -Cp(CO)(L)FeMe⁺ in methylene chloride containing 0.1 M TBAH at 0 °C under 1 atm of CO.
^d E° values (mV) in methylene chloride containing 0.1 M TBAH at 0 °C for the η -Cp(CO)(L)FeMe/ η -Cp(CO)(L)FeMe⁺ couple measured relative to acetylferrocene, which was used as an internal standard. The E° values measured by square-wave and cyclic voltammetry agree within 2 mV. The error in each measurement is ± 2 mV.

Table II. Activation Parameters for the Carbonylation of Two Complexes, η -Cp(CO)(L)FeMe⁺, in Methylene Chloride Containing 0.1 M TBAH under 1 atm of CO at 0 °C

L	ΔH^{\ddagger} , kcal/mol	ΔS^{\ddagger} , eu
P(<i>p</i> -ClPh) ₃	7.8 \pm 2.0	-23 \pm 7
P(<i>p</i> -CF ₃ Ph) ₃	6.7 \pm 0.8	-25 \pm 3

rameters for the carbonylation of two of the iron(III) triarylphosphine complexes are displayed in Table II.

$$d[\eta\text{-Cp(CO)(L)FeCOMe}^+]/dt = k_{mi}[\eta\text{-Cp(CO)(L)FeMe}^+] \quad (9)$$

The stereochemical studies show that the redox-catalyzed carbonylation of (+)- η -Cp(CO)(PPh₃)FeMe yields racemic η -Cp(CO)(PPh₃)FeMe. Control experiments demonstrated that (+)- η -Cp(CO)(PPh₃)FeMe racemized under similar conditions in the absence of carbon monoxide. Redox-catalyzed carbonylation of η -Cp(CO)(PPh₃)FeMe in the presence of ¹³CO affords η -Cp(¹³CO)(PPh₃)FeCOMe. There was no evidence for incorporation of ¹³CO into the residual η -Cp(CO)(PPh₃)FeMe or into the acyl position of the iron(II) acyl complex.

The kinetic data were analyzed by the quantitative analysis of ligand effects (QALE).^{17,18} QALE involves the construction of electronic and steric profiles. An electronic profile is the plot of log k_{mi} versus χ , which is a measure of the electron-donor capacity of the phosphorus(III) ligand.^{17b} Steric profiles are plots of the deviation, log k_{st} ,

(17) (a) Liu, H.-Y.; Eriks, E.; Prock, A.; Giering, W. P. *Acta Crystallogr.* 1990, C46, 51-54. (b) Panek, J.; Prock, A.; Eriks, K.; Giering, W. P. *Organometallics* 1990, 9, 2175. (c) Liu, H.-Y.; Eriks, E.; Prock, A.; Giering, W. P. *Organometallics* 1990, 9, 1758. (d) Eriks, K.; Liu, H.-Y.; Koh, L.; Prock, A.; Giering, W. P. *Acta Crystallogr.* 1989, C45, 1683-86. (e) Rahman, Md. M.; Liu, H.-Y.; Eriks, K.; Prock, A.; Giering, W. P. *Organometallics* 1989, 8, 1-7. (f) Eriks, K.; Liu, H.-Y.; Prock, A.; Giering, W. P. *Inorg. Chem.* 1989, 28, 1759-63. (g) Rahman, Md. M.; Liu, H.-Y.; Prock, A.; Giering, W. P. *Organometallics* 1987, 6, 650-58. (h) Golovin, M. N.; Rahman, Md. M.; Belmonte, J. E.; Giering, W. P. *Organometallics* 1985, 4, 1981-91.

(18) (a) Lezhan, C.; Poe, A. J. *Inorg. Chem.* 1989, 28, 3641. (b) Brodie, N. M.; Chen, L.; Poe, A. J. *Int. Nat. J. Kinet.* 1988, 27, 188. (c) Poe, A. J. *Pure Appl. Chem.* 1988, 60, 1209. (d) Dahlinger, K.; Falcone, F.; Poe, A. J. *Inorg. Chem.* 1986, 25, 2654.

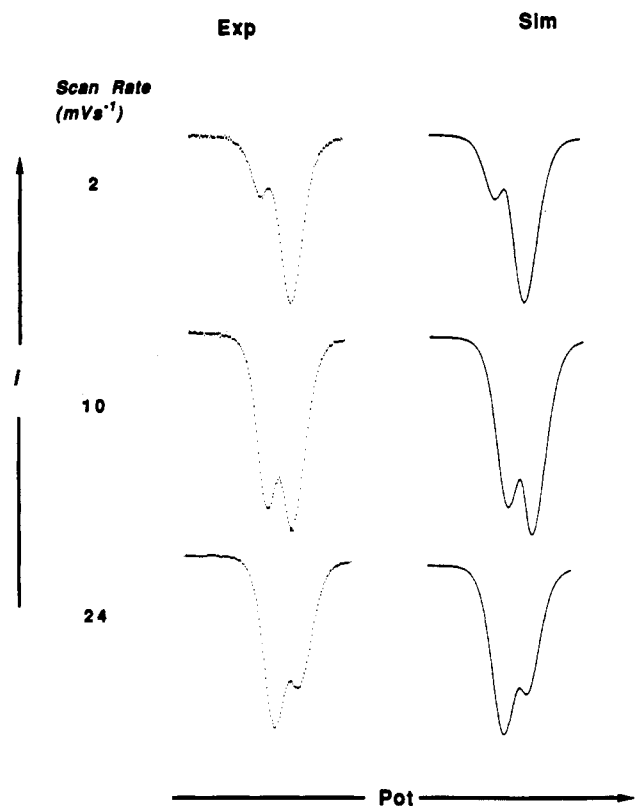


Figure 2. Experimental and simulated square-wave voltammograms for the oxidation of η -Cp(CO)(P(*p*-CF₃Ph)₃)FeMe under 1 atm of carbon monoxide containing 0.1 M TBAH at 0 °C. The voltammograms were obtained by sweeping the potential in the positive direction. The first wave corresponds to the oxidation of η -Cp(CO)(P(*p*-CF₃Ph)₃)FeMe and the second to the oxidation of η -Cp(CO)(P(*p*-CF₃Ph)₃)FeCOMe formed during the experiment.

of data in the electronic profile from the line (determined by isosteric steric ligands or small ligands that exhibit no steric effects) versus cone angle, θ , of the ligand, L. The electronic profile displayed in Figure 3 shows that the rate of carbonylation of η -Cp(CO)(L)FeMe⁺ increases as the electron-donor capacity of L decreases, with η -Cp(CO)(P(*p*-CF₃Ph)₃)FeMe⁺ being the most reactive member of the set. The steric profile (Figure 3) shows a region of steric inhibition for small ligands followed by a steric threshold near $\theta = 150^\circ$, which ushers in a region of steric acceleration. Analysis of the E° values for the η -Cp(CO)(L)-FeMe/ η -Cp(CO)(L)FeMe⁺ (Table I) couple reveals a region of no steric effects for $\theta < 149^\circ$, a steric threshold near 150° after which the E° values move to more positive potentials (eq 10).

$$E^{\circ} \text{ (mV)} = (23.8 \pm 0.8)\chi + (2.73 \pm 0.59)(\theta - 149^\circ) - (690 \pm 10) \quad (10)$$

$$r = 0.997$$

Discussion

The impetus for this research was to understand the dramatic increase in the rate of carbonylation of the Fe-Me bond on going from the iron(II) to the iron(III) state. In order to gain this insight, we have probed the intimate details of the carbonylation of η -Cp(CO)(L)FeMe⁺ as a function of the ancillary ligand, L.

The lack of kinetic dependence of the carbonylation of η -Cp(CO)(L)FeMe⁺ on [CO] demonstrates that the rate-determining step is the transformation of η -Cp(CO)(L)-FeMe⁺ to a transient intermediate followed by the rapid reaction with CO. There are two reasonable choices for

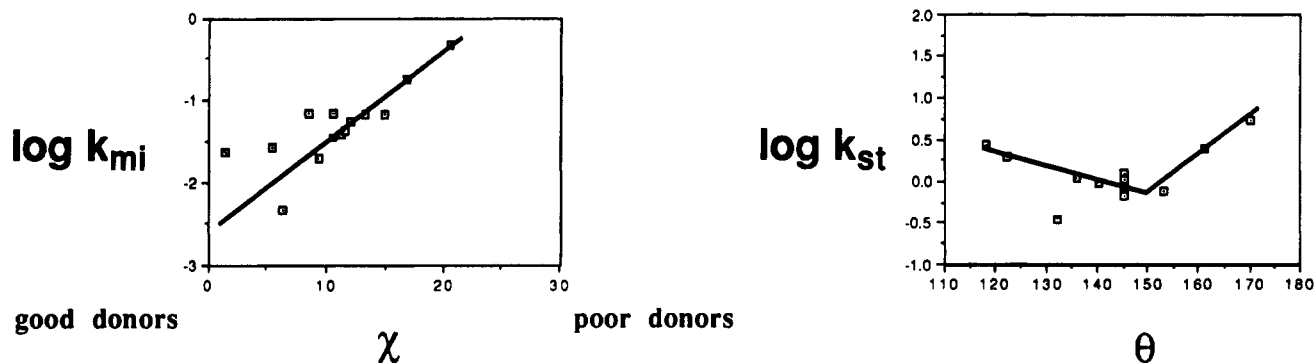
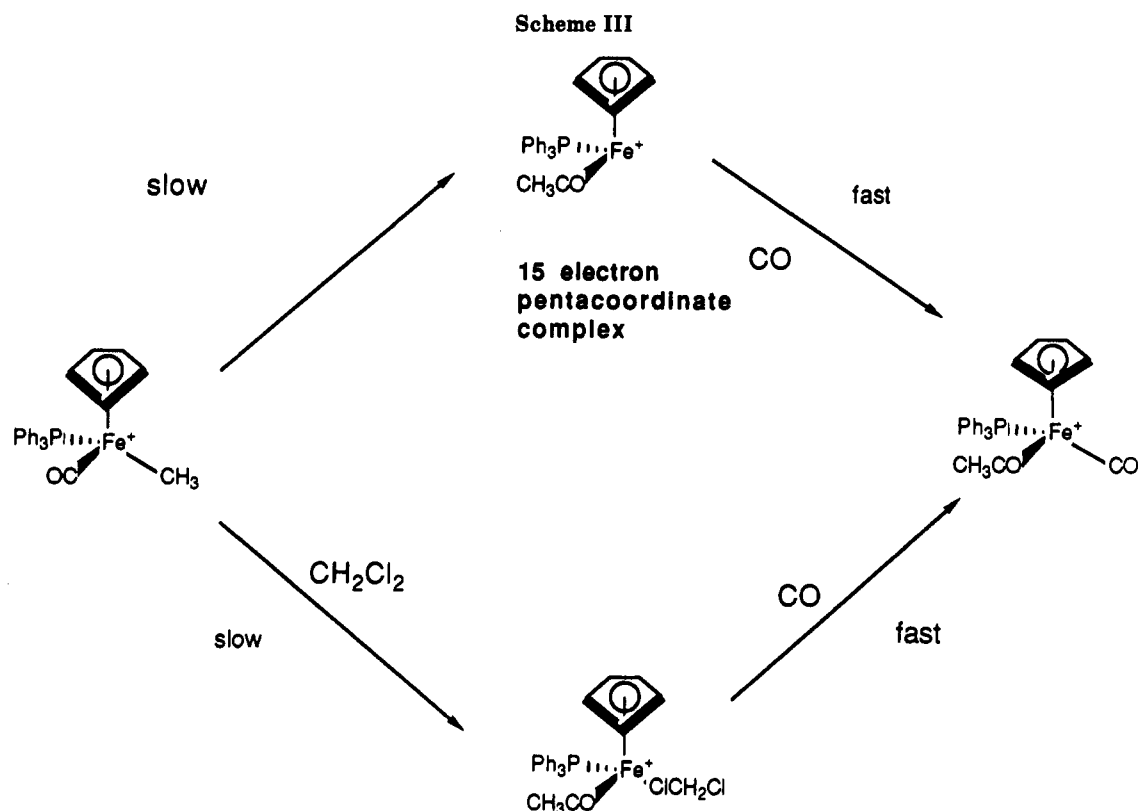


Figure 3. Electronic (left) and steric (right) profiles for the carbonylation of the $\eta\text{-Cp}(\text{CH}_2\text{Cl}_2)(\text{L})\text{FeCOMe}^+$ in methylene chloride at 0 °C under 1 atm of carbon monoxide. Profiles were constructed from the data displayed in Table I. Line is drawn through the points for the complexes containing the isosteric ($\theta = 145^\circ$) para-substituted triarylphosphine ligands. $\log k_{st}$ is the vertical deviation of the other points from this line.



this intermediate: a coordinatively unsaturated 15-electron species $\eta\text{-Cp}(\text{L})\text{FeCOMe}^+$ or a solvent (CH_2Cl_2) or anion (PF_6^-) coordinated acyl complex such as $\eta\text{-Cp}(\text{CH}_2\text{Cl}_2)(\text{L})\text{FeCOMe}^+$ or $\eta\text{-Cp}(\text{PF}_6)(\text{L})\text{FeCOMe}$ (Scheme III). Some of the evidence (labeling experiments, stereochemistry, kinetics, and nucleophilic enhancement and inhibition (vide infra)) is consistent with either intermediate. The observation of the large negative entropy of activation ($\Delta S^\ddagger = -23$ to -25 eu), however, militates for the involvement of the solvent or solute. The size of ΔS^\ddagger is similar to that observed for other solvent-assisted alkyl to acyl migratory insertion reactions.¹⁹ Even though we show the intermediate as $\eta\text{-Cp}(\text{CH}_2\text{Cl}_2)(\text{L})\text{FeCOMe}^+$, we cannot exclude $\eta\text{-Cp}(\text{PF}_6)(\text{L})\text{FeCOMe}$, which might be formed from a tight ion pair. (We must point out at this juncture that the reaction is very sensitive to nucleophilic catalysis; accordingly, we cannot rule out the possibility that the nucleophilic catalyst is an impurity in the solvent or the

supporting electrolyte. However, we do obtain reproducible results when samples are prepared as described in the Experimental Section.) In either case, we believe that the alkyl to acyl migratory insertion reaction is a nucleophile-assisted process. In order to probe further these issues, we are currently conducting experiments in less coordinating solvents with very weakly nucleophilic solutes.

Analysis of the kinetic and electrochemical data allows us to gain insight into the nature of the transition state. The coordination of solvent requires the transition state of the rate-determining step to be formally heptacoordinate and possibly electron rich compared to the ground state. The electronic profile (Figure 3) shows that the reaction accelerates as the electron-donor capacity of L diminishes (larger χ). It seems likely that a heptacoordinate transition state would be more crowded than the ground state. Under these conditions the rate of reaction should fall as the size of L increases. The steric profile (Figure 3) does show a region of steric inhibition (118–150°), but this followed by a region of steric acceleration as the size of L increases.²⁰ Although we have not seen this type of steric

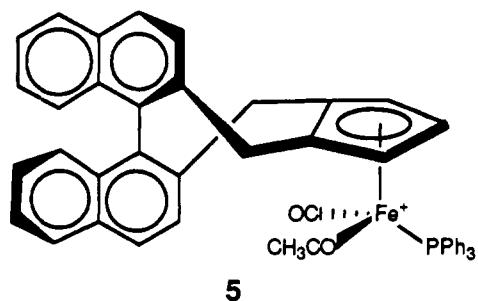
(19) Cotton, J. D.; Crisp, G. T.; Laitif, L. *Inorg. Chim. Acta* 1981, 47, 171.

profile previously, it is one of four general types that we proposed earlier.^{17f} In order to produce this steric profile, the reaction must possess a transition state that is more crowded but less rigid than the ground state. Thus, for $\theta < 150^\circ$ the transition-state energy is slowly rising while the ground-state energy is not significantly perturbed by the increasing size of L. After 150° the ground state becomes sterically destabilized. The ground state must be more rigid and its energy must rise more rapidly than that of the transition state since the reaction becomes sterically accelerated in this domain. Since η -Cp(CH₂Cl₂)(L)Fe-COMe⁺ is not observable, the equilibrium constant for its formation must be small and the Fe-ClCH₂Cl bond must be weak. Thus, it appears to us that the transition state probably involves a weakly bonded entering nucleophile (CH₂Cl₂ or PF₆⁻) and extensively rearranged methyl and terminal carbonyl ligands.

If the steric threshold at 150° is attributable to the onset of steric destabilization in η -Cp(CO)(L)FeMe⁺, then this phenomenon should be observable by nonkinetic methods. Indeed, the analysis of the E° values for the η -Cp(CO)(L)FeMe/ η -Cp(CO)(L)FeMe⁺ couple clearly shows a steric threshold at 149° (eq 10). Since the E° values move to higher potentials as the size of the ligand increases after the threshold, it is clear that η -Cp(CO)(L)FeMe⁺ is being sterically destabilized relative to η -Cp(CO)(L)FeMe. As far as we know, this is the first example of the same steric threshold being observed in both kinetic and thermodynamic data.

Based on studies of the carbonylation process in acetonitrile, which involves rate-determining displacement of the solvent ligand by carbon monoxide, we believe that the subsequent reaction between η -Cp(CH₂Cl₂)(L)FeCOMe⁺ is a concerted displacement of the solvent ligand by CO. This mechanism accounts for the exclusive incorporation of ¹³CO at the terminal position of η -Cp(¹³CO)(PPh₃)FeCOMe⁺. The formation of racemic η -Cp(CO)(PPh₃)FeCOMe from (+)- η -Cp(CO)(PPh₃)FeMe is problematic. It appears that the racemization occurs before the formation of η -Cp(CO)(PPh₃)FeCOMe⁺ since Halterman and Colletti²¹ have found that the chiral acetyl complex (5) is configurationally stable when treated with ferrocenium

hexafluorophosphate at 0 °C. Furthermore, (+)- η -Cp-



(CO)(PPh₃)FeMe is rapidly racemized by 5 mol % ferrocenium tetrafluoroborate in methylene chloride under an atmosphere of argon. Thus, the racemization process does not necessarily involve CO. Therefore, it appears that racemization occurs either during the formation of η -Cp(CH₂Cl₂)(L)FeCOMe⁺ or by solvent ligand/solvent ligand exchange reactions of η -Cp(CH₂Cl₂)(L)FeCOMe⁺. We are not aware of any studies of the stereochemistry of these weakly solvent coordinated acyl complexes.

Conclusions

The alkyl to acyl migratory insertion reaction in η -Cp(CO)(L)FeMe⁺ is nucleophilically assisted and probably does not involve the intermediacy of the coordinatively unsaturated 15-electron complexes, η -Cp(L)FeCOMe⁺. The transition state might resemble η -Cp(L)FeCOMe⁺, however, with extensively rearranged methyl and terminal carbonyl ligands and the nucleophile just entering the coordination sphere of the metal. Since the nucleophile contributes little stability to the transition state, the high rate of the alkyl to acyl migratory insertion reaction is probably associated with preferential ground-state destabilization associated with weakening of the Fe-CO bond in the Fe(III) state.

Acknowledgment. We gratefully acknowledge the donors of the Petroleum Research Fund, administered by the American Chemical Society, for support of this work. Also, we thank Professor Ronald Halterman (Boston University) for stimulating discussions and for sharing unpublished results from his laboratory.

Supplementary Material Available: IBM 7090 computer program used in experimental simulations (2 pages). Ordering information is given on any current masthead page.

(20) The datum for the triethylphosphine complex falls far off the steric profile. This might be attributable to entropic conformational effects associated with alkyl groups. Brown, H. C.; Taylor, M. D.; Sujishi, S. *J. Am. Chem. Soc.* 1951, 73, 2464.

(21) Halterman, R.; Colletti, S. Unpublished results.